



Reliability based modeling of hybrid solar/wind power system for long term performance assessment

Serkan Eryilmaz^{a,*}, İrem Bulanık^a, Yilser Devrim^b

^a Atılım University, Department of Industrial Engineering, Ankara, Turkey

^b Atılım University, Department of Energy Systems Engineering, Ankara, Turkey

ARTICLE INFO

Keywords:

Expected energy not supplied
Hybrid system
Renewable energy
Wind speed
Wind turbine

ABSTRACT

This paper is concerned with reliability based long-term performance assessment of hybrid solar/wind power system. In particular, an analytical expression is obtained for the theoretical distribution of the power output of the hybrid system by taking into account the reliability values of renewable energy components. An expression for the expected energy not supplied (EENS) is also derived and used to compute the energy index of reliability (EIR) that is directly related to EENS. Because the derived expressions involve reliability values which are related to mechanical states of the renewable energy components, the results enable us to evaluate properly the performance of the hybrid system. A numerical example is included to illustrate the results.

1. Introduction

In recent years, the use of renewable energy for electricity generation has intensified due to the increase in fossil fuel prices, environmental pollution and their limited nature [1,2]. On the contrary, renewable energy sources are the most promising alternative energy sources due to their continuity, availability from nature and their rich and clean properties. However, the major disadvantages of renewable energy sources are their intermittent nature. Besides, seasonal climate and geographical conditions affect wind and solar energy production [3]. For this reason, combining two or more renewable energy sources provides more secure and continuous electricity production. Hybrid renewable energy systems are used to eliminate the disadvantages of the variability and randomness of a single renewable energy source [4]. Hybrid energy systems that use both solar and wind sources together are more advantageous than only solar or wind energy based systems since they have high system efficiency and power reliability.

When we talk about reliability in the context of power systems, two different reliability concepts should be considered. In general, the reliability is the probability that a system will perform satisfactorily for at least a given period of time when it is used under stated conditions. Consider a wind turbine (WT) as a power system. It produces power when it mechanically works and the wind speed is at a required level. When a failure occurs, the WT cannot produce power even if the wind speed is enough for power production. Thus, the overall reliability of the wind turbine must be evaluated by taking into account both its mechanical failure/operation and the wind speed which is

an external source of randomness. The former is related to security assessment while the latter one is concerned with adequacy assessment. To make more clear the concepts, consider one of the most commonly used reliability measures of power systems. The Expected Energy not Supplied (EENS) is defined to be the expected energy that will not be supplied when the local load L exceeds the available generation. Thus, $EIR = 1 - \frac{EENS}{L}$ which is called Energy Index of Reliability is used as a reliability index. However, when we consider the reliability of the wind turbine that is modeled with two mechanical states: complete failure and perfect functioning, under very general assumptions, it can be expressed as

$$P\{X = 1\} = \frac{\mu}{\mu + \lambda}, \quad (1)$$

where X denotes the mechanical state of the WT as $X = 1$ if it works, and $X = 0$ if it fails, the parameters λ and μ represent respectively the failure and repair rates of the WT (see, e.g. Li and Zio [5]). Throughout the paper, the reliability value $P\{X = 1\}$ is assumed to be given. That is, it is not the aim of this paper to compute $P\{X = 1\}$. There is an extensive literature on reliability evaluation of wind turbines. Not only simple Markov model that yields (1) but also more complicated models considering time dependent deterioration of the WT have been investigated in the literature. The interested reader may refer to Spinato et al. [6], Guo et al. [7], Scheu et al. [8].

To have a more accurate metric for reliability of the power system, the reliability of the WT which is defined by (1) should also be

* Corresponding author.

E-mail addresses: serkan.eryilmaz@atilim.edu.tr (S. Eryilmaz), irem.bulanik@atilim.edu.tr (İ. Bulanık), yilser.devrim@atilim.edu.tr (Y. Devrim).

Nomenclature

V	Wind speed random variable (m s^{-1})
$f(v)$	The probability density function (pdf) of V
$F(v)$	The cumulative distribution function (cdf) of V
S	Solar irradiation (kW/m^2)
$g(s)$	The pdf of S
$G(s)$	The cdf of S
v_{ci}	The cut-in wind speed (m s^{-1})
v_r	The rated wind speed (m s^{-1})
v_{co}	The cut-out wind speed (m s^{-1})
P_r	The rated power of a single wind turbine (kW)
P_{WT}	The power generated by the wind turbine (kW)
p_1	The reliability of the wind turbine (WT)
A_{PV}	PV array surface area (m^2)
P_{PV}	The power output of the photovoltaic system (PVS)
η_{PV}	The efficiency of the PVS
p_2	The reliability of the PVS
$Q(x)$	The cdf of the power produced by the WT
$R(x)$	The cdf of the power produced by the PVS
μ_{WT}	The mean power produced by WT (kW)
μ_{PV}	The mean power produced by PVS (kW)
P_h	The power output of the hybrid solar-wind power system (HSWPS) (kW)
μ_h	The mean power generated by HSWPS (kW)

considered and involved in performance characteristics of the power system. For example, the *EENS* should be formulated as

$$EENS = E(\max(L - P_{WT} \cdot X, 0)), \quad (2)$$

where $E(\cdot)$ denotes the expected value operator, P_{WT} is the power generated by the wind turbine which is also a random variable since it depends on the wind speed. The random variable $\max(L - P_{WT} \cdot X, 0)$ represents the demand that the system (WT) is unable to serve as a result of loss of load event, and $\max(L - P_{WT} \cdot X, 0) \equiv L - P_{WT} \cdot X$ if $L - P_{WT} \cdot X > 0$ and $\max(L - P_{WT} \cdot X, 0) \equiv 0$ if $L - P_{WT} \cdot X \leq 0$. Such a formulation yields

$$EIR = 1 - \frac{E(\max(L - P_{WT} \cdot X, 0))}{L} \quad (3)$$

which becomes now dependent on reliability $P\{X = 1\}$ of the WT.

The probabilistic analysis of wind and/or solar energy systems is essential since these systems have stochastic nature. Various probabilistic models have been constructed and solved for renewable energy systems. Barros et al. [9] presented probabilistic models to assess the costs of power plants. Faza [10] evaluated the effect of adding photovoltaic sources from a reliability perspective. Hasan et al. [11] provided a critical assessment and classification of the available probabilistic computational methods that have been applied to power system stability assessment. Kan et al. [12] studied the theoretical distribution of the wind farm power when there is a correlation between wind speed and wind turbine availability. Adedipe et al. [13] provided a review and evaluation of existing research on the use of Bayesian Network models in the wind energy sector.

Combining wind and solar energies in a hybrid system provides a more reliable system in terms of power generation. Such a hybrid system has been extensively considered and studied in the literature

from various perspectives. Li and Zio [5] established multi-state hybrid systems and computed reliability indices such as loss of load expectation (LOLE) and expected energy not supplied via universal generating functions. Acuña et al. [14] introduced a new reliability indicator that is based on the minimum of the outputs of photovoltaic and wind systems, and established a multi-objective optimization problem using this indicator. Kamal Anoune et al. [15] presented an extensive review on sizing methods and optimization techniques for PV-wind based hybrid renewable energy system. Moghaddam et al. [16] established an optimization problem that is based on LOLE for a hybrid system including PV panels, wind turbine and fuel cell to minimize the total net present cost. Devrim and Eryilmaz [17] modeled a hybrid system that consists of a specified number of wind turbines and solar modules as a threshold system.

In this paper, we deal with a hybrid solar/wind power system and evaluate its performance by considering reliability values of renewable energy components. In particular, we obtain the theoretical distribution of the power generated by a hybrid system which is equal to the power output of the WT plus the power output of the (photovoltaic system) PVS. The results are then used to compute the EENS and EIR for the hybrid system. The theoretical distribution of the power of the hybrid system that consists of n identical WTs and PVS is also derived. As far as we know, this practically important setting allowing for more adequate performance assessment of the hybrid system was not considered in the literature. The theoretical results are illustrated using the data that is obtained from Meteororm software for a specific location.

The paper is organized as follows. In Section 2, we present the notation and main definitions that will be used throughout the paper. Section 3 is devoted to the derivation of the theoretical distribution of the aggregate power produced by the hybrid system. In Section 4, an expression for the EENS that is based on the distribution of the power of the hybrid system is obtained. Section 5 contains numerical results.

2. Definitions and notation

In this section, we present the definitions that will be used throughout the paper.

For a fixed wind speed $V = v$, the well-known relationship between the wind speed and the power generated by WT is given by (4) (see, e.g. Louie and Slougher [18]).

$$P_{WT} = \begin{cases} 0, & \text{if } v < v_{ci} \text{ or } v \geq v_{co} \\ P_r \frac{(v^3 - v_{ci}^3)}{(v_r^3 - v_{ci}^3)}, & \text{if } v_{ci} \leq v < v_r \\ P_r, & \text{if } v_r \leq v < v_{co} \end{cases} \quad (4)$$

The reason for choosing P_{WT} is twofold. First, Eq. (4) involves WT characteristics v_{ci} , v_r , v_{co} and P_r . Second, based on detailed analysis on the relationship between the wind speed and the WT output values, the cubic relationship has been found to be accurate in various cases (see, e.g. [19]).

Let $Q(x) = P\{P_{WT} \leq x\}$ be the cdf of the power produced by WT. Then,

$$Q(x) = \begin{cases} 0, & \text{if } x < 0 \\ H(x), & \text{if } 0 \leq x < P_r \\ 1, & \text{if } x \geq P_r, \end{cases} \quad (5)$$

where

$$H(x) = 1 - F(v_{co}) + F\left[\left[\frac{x}{P_r}(v_r^3 - v_{ci}^3) + v_{ci}^3\right]^{\frac{1}{3}}\right]. \quad (6)$$

For the fixed solar irradiation $S = s$ (kW/m^2), the basic equation for the power output of the PVS is

$$P_{PV} = S \cdot \eta_{PV} \cdot A_{PV}, \quad (7)$$

where A_{PV} is the module area and η_{PV} is the electrical efficiency of the module. The cdf of P_{PV} can be computed from

$$R(x) = P \{ P_{PV} \leq x \} = P \left\{ S \leq \frac{x}{\eta_{PV} \cdot A_{PV}} \right\} = G\left(\frac{x}{\eta_{PV} \cdot A_{PV}}\right), \quad (8)$$

for $0 < x < \eta_{PV} \cdot A_{PV}$.

3. The power of the hybrid system

In this section, we derive the theoretical distribution of the aggregate power produced by the hybrid system. We first consider the case when the system has only one WT. Then, the result is generalized to the case when there are n identical WTs. The case of n identical WTs is first considered here.

3.1. The system with a single WT

The power generated by the hybrid system P_h is equal to the power output of the WT plus the power output of the PVS. That is,

$$P_h = X \cdot P_{WT} + Y \cdot P_{PV}, \quad (9)$$

where X and Y are binary random variables that respectively represent mechanical states of the WT and PVS. The probabilities $p_1 = P \{ X = 1 \}$ and $p_2 = P \{ Y = 1 \}$ denote respectively the reliabilities of WT and PVS. It is not the aim of this paper to compute and evaluate reliability values p_1 and p_2 . They are assumed to be given. There have been numerous studies to investigate reliability of wind turbine and photovoltaic system (see, e.g. [20,21]).

Considering all possible mechanical states of the WT and PV, for $x \geq 0$, we have

$$P \{ P_h \leq x \} = p_1 p_2 P \{ P_{WT} + P_{PV} \leq x \} + p_1 (1 - p_2) P \{ P_{WT} \leq x \} + (1 - p_1) p_2 P \{ P_{PV} \leq x \} + (1 - p_1)(1 - p_2). \quad (10)$$

The first term on the right hand side of Eq. (10) corresponds to the case when both WT and PV are in working states. The second (third) term represents the case when WT (PV) is working and PV (WT) has failed. Finally, $(1 - p_1)(1 - p_2)$ is the probability that neither WT nor PV is working. To obtain an expression for the cdf of P_h , we need the cdfs of P_{WT} , P_{PV} and $P_{WT} + P_{PV}$. The cdfs of P_{WT} and P_{PV} are given respectively by (5) and (8). Let $K(x) = P \{ P_{WT} + P_{PV} \leq x \}$. Then, (see Appendix)

$$K(x) = \begin{cases} 0, & \text{if } x < 0 \\ \int_0^{\min(\frac{x}{\eta_{PV} A_{PV}}, 1)} T_F(x, s) g(s) ds, & \text{if } 0 \leq x < P_r \\ \int_{\frac{x-P_r}{\eta_{PV} A_{PV}}}^{\min(\frac{x}{\eta_{PV} A_{PV}}, 1)} T_F(x, s) g(s) ds + G\left(\frac{x - P_r}{\eta_{PV} A_{PV}}\right) & \text{if } P_r \leq x < \eta_{PV} A_{PV} + P_r \\ 1 & \text{if } x \geq \eta_{PV} A_{PV} + P_r \end{cases} \quad (11)$$

where

$$T_F(x, s) = 1 - F(v_{co}) + F \left[\left[\frac{x - s \eta_{PV} A_{PV}}{P_r} (v_r^3 - v_{ci}^3) + v_{ci}^3 \right]^{\frac{1}{3}} \right].$$

Thus, under reliability based model, the cdf of the power generated by the hybrid system is calculated from

$$P \{ P_h \leq x \} = p_1 p_2 K(x) + p_1 (1 - p_2) Q(x) + (1 - p_1) p_2 R(x) + (1 - p_1)(1 - p_2). \quad (12)$$

Tina et al. [22] derived the pdf corresponding to the distribution $K(x)$ under slightly different assumptions. First, their model does not take into account the reliability values of WT and PVS. Second, they have assumed a linear relationship between the wind speed and the power output of the WT. Our model is based on cubic relationship

as shown in (4). Third, their equation for modeling the power output of the PVS is more complicated and more accurate since it involves inclination, declination, and reflectance parameters etc. Since the basic model given by (7) is mathematically more tractable, we have preferred to use it as a starting point in our developments. On the other hand, the model used by Tina et al. [22] requires a detailed solar data which should consider inclination, declination etc.

The probability that the hybrid system produces no power can be computed from

$$P \{ P_h = 0 \} = P \{ X = 0, Y = 0 \} + P \{ X = 1, Y = 0, V < v_{ci} \text{ or } V \geq v_{co} \} = (1 - p_1)(1 - p_2) + p_1(1 - p_2) [1 - F(v_{co}) + F(v_{ci})]. \quad (13)$$

In the derivation process of (12), we did not make any assumption on wind speed and solar irradiation distributions. That is, we can calculate the cdf given by (12) for arbitrarily chosen F and G .

Using (9), the mean power produced by the hybrid system is found to be

$$\mu_h = p_1 \mu_{WT} + p_2 \mu_{PV}, \quad (14)$$

where

$$\begin{aligned} \mu_{WT} &= \int_0^{P_r} (1 - H(x)) dx \\ &= \int_0^{P_r} \left[F(v_{co}) - F \left(\left[\frac{x}{P_r} (v_r^3 - v_{ci}^3) + v_{ci}^3 \right]^{\frac{1}{3}} \right) \right] dx \\ &= P_r F(v_{co}) - \int_0^{P_r} F \left(\left[\frac{x}{P_r} (v_r^3 - v_{ci}^3) + v_{ci}^3 \right]^{\frac{1}{3}} \right) dx, \end{aligned} \quad (15)$$

and

$$\mu_{PV} = \eta_{PV} \cdot A_{PV} \cdot E(S) = \eta_{PV} \cdot A_{PV} \int_0^1 s g(s) ds. \quad (16)$$

3.2. The system with n identical WTs

For the hybrid system consisting of n identical WTs, the power output of the system can be expressed as

$$P_h = S_n \cdot P_{WT} + Y \cdot P_{PV}, \quad (17)$$

where S_n is the total number of available (working) WTs. Clearly,

$$P \{ S_n = i \} = \binom{n}{i} p_1^i (1 - p_1)^{n-i}, \quad (18)$$

for $i = 0, 1, \dots, n$.

By conditioning on the number of available WTs, for $x \geq 0$, we obtain

$$\begin{aligned} P \{ P_h \leq x \} &= \sum_{i=1}^n \binom{n}{i} p_1^i (1 - p_1)^{n-i} p_2 P \{ i \cdot P_{WT} + P_{PV} \leq x \} \\ &\quad + \sum_{i=1}^n \binom{n}{i} p_1^i (1 - p_1)^{n-i} (1 - p_2) P \{ i \cdot P_{WT} \leq x \} \\ &\quad + (1 - p_1)^n p_2 P \{ P_{PV} \leq x \} + (1 - p_1)^n (1 - p_2). \end{aligned} \quad (19)$$

Let $Q_i(x) = P \{ i \cdot P_{WT} \leq x \}$. Then, from Eryilmaz and Devrim [23], we have

$$Q_i(x) = \begin{cases} 0, & \text{if } x < 0 \\ H_i(x), & \text{if } 0 \leq x < iP_r \\ 1, & \text{if } x \geq iP_r, \end{cases} \quad (20)$$

where

$$H_i(x) = 1 - F(v_{co}) + F \left[\left[\frac{x}{iP_r} (v_r^3 - v_{ci}^3) + v_{ci}^3 \right]^{\frac{1}{3}} \right].$$

On the other hand, for $i \geq 1$, when there are i available WTs, we have

$$K_i(x) = P \{i \cdot P_{WT} + P_{PV} \leq x\} = \int_0^1 Q_i(x - s \cdot \eta_{PV} \cdot A_{PV})g(s)ds.$$

Following the same steps that have been considered for single WT,

$$K_i(x) = \begin{cases} 0, & \text{if } x < 0 \\ \int_0^{\min(\frac{x}{\eta_{PV} A_{PV}}, 1)} Z_F(x, s, i)g(s)ds, & \text{if } 0 \leq x < iP_r \\ \int_{\frac{x-iP_r}{\eta_{PV} A_{PV}}}^{\min(\frac{x}{\eta_{PV} A_{PV}}, 1)} Z_F(x, s, i)g(s)ds + G(\frac{x-iP_r}{\eta_{PV} A_{PV}}) & \text{if } iP_r \leq x < \eta_{PV} A_{PV} + iP_r \\ 1 & \text{if } x \geq \eta_{PV} A_{PV} + iP_r, \end{cases} \quad (21)$$

where

$$Z_F(x, s, i) = 1 - F(v_{co}) + F\left[\left[\frac{x - s\eta_{PV} A_{PV}}{iP_r}(v_r^3 - v_{ci}^3) + v_{ci}^3\right]^{\frac{1}{3}}\right].$$

Thus, the distribution of the hybrid system consisting of n WTs is obtained by substituting (8), (20) and (21) in (19).

The mean power produced by the hybrid system is found to be

$$\mu_h = n p_1 \mu_{WT} + p_2 \mu_{PV}, \quad (22)$$

where μ_{WT} and μ_{PV} are given respectively by (15) and (16).

4. Expected energy not supplied

EENS is one of the most commonly used indices in reliability evaluation of power systems. It is defined to be the expected energy that will not be supplied when the local load exceeds the available generation. For a local load L , it can be defined by the expected value

$$EENS = E(\max(L - P_h, 0)).$$

Tina et al. [22] obtained expression for the $EENS$ which is based on the pdf of P_h . Below, we obtain alternative expression that is based on the cdf of the power output of the hybrid system. It is more practical to use this formula if the cdf is available. If $P_{h\max}$ (which is equal to $P_r + \eta_{PV} \cdot A_{PV}$ in our setup) denotes the maximum power generated by the hybrid system, then (see Appendix)

$$EENS = L - \int_0^{\min(L, P_{h\max})} P \{P_h \geq u\} du. \quad (23)$$

For the hybrid system under concern, by substituting (12) in (23), we obtain (see Appendix)

$$EENS = L - p_1 p_2 \int_0^{\min(L, P_{h\max})} [1 - K(u)] du - p_1 (1 - p_2) \int_0^{\min(L, P_r)} [1 - Q(u)] du - (1 - p_1) p_2 \int_0^{\min(L, \eta_{PV} A_{PV})} [1 - R(u)] du. \quad (24)$$

The expression (24) is general as it is also useful to compute the EENS for the system which is established only by a WT or PVS. Indeed, if $p_2 = 0$, then the EENS for a single WT becomes

$$EENS = L - p_1 \int_0^{\min(L, P_r)} [1 - Q(u)] du. \quad (25)$$

For a PVS, choosing $p_1 = 0$ in (24) one obtains

$$EENS = L - p_2 \int_0^{\min(L, \eta_{PV} A_{PV})} [1 - R(u)] du. \quad (26)$$

For a hybrid system that consists of n identical WTs, the EENS can be computed by substituting (19) in (23). In this case, we have

$$EENS = L - \int_0^{\min(L, nP_r + \eta_{PV} A_{PV})} (1 - P \{P_h \leq u\}) du,$$

where $P \{P_h \leq u\}$ is given by (19).

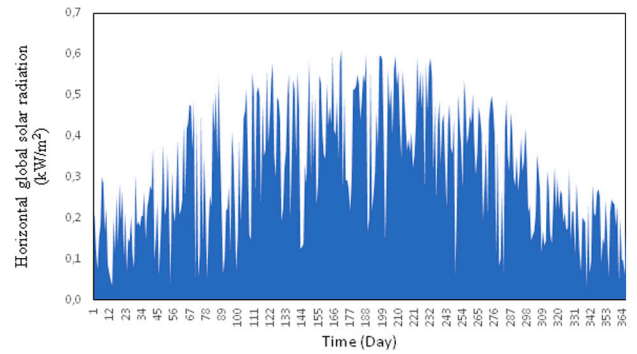


Fig. 1. Horizontal global solar irradiation for School of Foreign Languages of Atilim University.

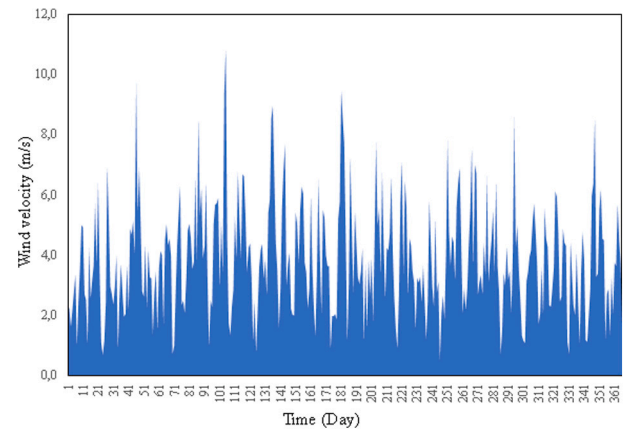


Fig. 2. Wind speed values at School of Foreign Languages of Atilim University.

5. Numerical example

Our numerical evaluations are based on the meteorology data that were taken for School of Foreign Languages of Atilim University (39.813°N, 32.726 °E) from Meteornorm software. Meteornorm is a unique combination of reliable data sources and sophisticated calculation tools. In this study, 2020 meteorology (predicted) data were obtained from Meteornorm with IPCC AR4 B1 scenario. The horizontal global solar irradiation and wind speed values of location are given respectively in Figs. 1 and 2. The data on wind speed is obtained during the whole day while the solar data depends on the daylight hours. Therefore, to obtain the solar irradiation data in a more accurate way, the solar radiation data is divided by the day length. That is, solar irradiation=(solar radiation)/day length.

For a specific month, wind speed was fitted to Weibull distribution whose cumulative distribution function is

$$F(v) = 1 - e^{-\left(\frac{v}{\hat{\alpha}}\right)^\beta}, \quad (27)$$

$v > 0$. The null hypothesis that the wind speed data comes from a Weibull distribution with cdf (27) has not been rejected at the 5% significance level using Kolmogorov–Smirnov (KS) goodness of fit test. The maximum likelihood estimators of the parameters of wind speed are computed and presented in Table 1 along with the estimated mean wind speed and the p -values of the KS test. The p -value is used whether the null hypothesis that the data comes from Weibull distribution is acceptable or not. In Table 1, all p -values are greater than the significance level 0.05. Thus, the wind speed data for each month may be modeled by Weibull distribution given by (27) with estimated values $\hat{\alpha}$ and $\hat{\beta}$.

Table 1
Point estimators of the parameters of the wind speed distribution.

	\hat{a} (m s ⁻¹)	$\hat{\beta}$ (m s ⁻¹)	Mean wind speed	p-value
January	3.5042	2.1042	3.1036	0.7884
February	4.0727	2.1490	3.6069	0.9616
March	4.5914	2.6797	4.0820	0.5900
April	5.2005	2.2259	4.6059	0.8935
May	4.6364	2.1109	4.1063	0.9525
June	4.6355	2.1187	4.1055	0.8368
July	4.6146	2.5706	4.0974	0.8972
August	4.0779	2.3996	3.6150	0.7288
September	4.6239	2.3601	4.0978	0.9044
October	4.0559	2.2631	3.5926	0.5356
November	4.0404	2.7225	3.5941	0.6479
December	4.0779	2.1458	3.6115	0.9812

Table 2
Point estimators of the parameters of the solar irradiation distribution.

	\hat{a} (kW/m ²)	\hat{b} (kW/m ²)	Mean solar radiation	p-value
January	3.5281	17.5253	0.1676	0.8569
February	4.5726	15.8676	0.2237	0.4475
March	2.1649	5.0689	0.2993	0.3347
April	3.4118	6.6326	0.3397	0.8363
May	4.2703	6.8737	0.3832	0.4542
June	7.5105	10.1842	0.4244	0.4243
July	5.2434	6.5615	0.4442	0.2320
August	10.0785	13.2440	0.4321	0.8882
September	6.0763	9.8249	0.3821	0.5319
October	3.7155	8.9574	0.2932	0.4965
November	6.6984	25.1371	0.2104	0.9071
December	3.5200	16.8736	0.1726	0.1185

Table 3
The values of input variables/parameters.

v_{ci}	v_r	v_{co}	P_r	A_{PV}	η_{PV}	p_1	p_2
2	11	21	5.5	1.63 · m	0.227	0.97	0.95

The Beta distribution whose probability density function is given by

$$g(s) = \frac{1}{B(a, b)} s^{a-1} (1-s)^{b-1}, \tag{28}$$

$0 < s < 1$ has been fitted to solar irradiation data, where $B(a, b)$ denotes Beta function. The KS test was applied to test the null hypothesis that the average daily solar irradiation data comes from Beta distribution with pdf given by (28). The results are presented in Table 2.

In the literature, Weibull and Beta distributions have been found to be suitable for modeling wind speed and solar irradiation data collected at many different locations. Based on the results in Tables 1 and 2, they are also suitable for the present data under concern. Although we have used these statistical distributions, our general equations can be used for any wind speed and solar irradiation distributions.

Based on the data presented in Tables 1 and 2, we compute EENS for each month when the load is fixed as 8 kW. The following information is necessary to compute the EENS:

1. The turbine characteristics v_{ci}, v_r, v_{co} and P_r
2. A_{PV} and η_{PV} values for the PVS
3. The reliability values p_1 and p_2 of WT and PVS

The PVS system is assumed to have m identical panels each have the area 1.63 m². Table 3 summarizes the input variables/parameters and their values.

The following two cases are considered:

Case 1: The HSWPS consists of $n = 1$ WT and the total area of PVS is 163 m².

Case 2: The HSWPS consists of $n = 3$ WTs and the total area of PVS is 130.4 m².

In Tables 4–5, we compute the mean output of the HSWPS and the EENS for each month for the cases 1 and 2, respectively. The mean

Table 4
The mean output, EENS and monthly EIR of the HSWPS for the Case 1.

	μ_{WT}^*	μ_{PV}^*	μ_h	EENS	EIR
January	0.1922	5.8905	6.0827	2.4982	0.6877
February	0.3088	7.8635	8.1723	1.3843	0.8270
March	0.3819	10.5198	10.9017	1.2479	0.8440
April	0.6440	11.9398	12.5838	0.7152	0.9106
May	0.4743	13.4696	13.9439	0.5433	0.9321
June	0.4724	14.9198	15.3922	0.3998	0.9500
July	0.3986	15.6130	16.0116	0.4328	0.9459
August	0.2806	15.1900	15.4706	0.3938	0.9508
September	0.4270	13.4322	13.8592	0.4607	0.9424
October	0.2900	10.3057	10.5957	0.9430	0.8821
November	0.2487	7.3960	7.6447	1.3772	0.8278
December	0.3106	6.0672	6.3778	2.3198	0.7100

Table 5
The mean output, EENS and monthly EIR of the HSWPS for the Case 2.

	μ_{WT}^*	μ_{PV}^*	μ_h	EENS	EIR
January	0.5766	4.7124	5.2890	2.9900	0.6262
February	0.9265	6.2908	7.2173	1.7360	0.7830
March	1.1457	8.4159	9.5616	1.3570	0.8304
April	1.9320	9.5518	11.4838	0.7590	0.9051
May	1.4230	10.7757	12.1987	0.5960	0.9255
June	1.4173	11.9358	13.3531	0.3920	0.9510
July	1.1958	12.4904	13.6862	0.4390	0.9451
August	0.8419	12.1520	12.9939	0.3870	0.9516
September	1.2809	10.7457	12.0266	0.4970	0.9379
October	0.8699	8.2446	9.1145	1.1600	0.8550
November	0.7462	5.9168	6.6630	1.8350	0.7706
December	0.9317	4.8537	5.7854	2.6640	0.6670

power $\mu_{WT}^* = n p_1 \mu_{WT}$ produced by the wind turbines and the mean power $\mu_{PV}^* = p_2 \mu_{PV}$ produced by the PVS are also included in the tables. Based on the results in Tables 4–5, we can conclude that the larger mean output of the HSWPS does not necessarily imply a smaller EENS. Indeed, although the mean power output of the system in July is larger when compared with the corresponding value in August, the EENS value is smaller for August. This supports the use of $EIR_m = 1 - \frac{EENS_m}{L}$ for a specific month m . A more fair comparison can be made based on EIR_m . From the Tables 4–5, we immediately observe that the HSWPS has the largest reliability value in August for both cases. The EENS values are mostly larger for the Case 1. However, there are some exceptional cases. For example, in June and August, the EENS values are larger for the Case 2. To assess the long term performance of the system, we can calculate yearly basis EIR which is

$$EIR_y = 1 - \frac{\sum_{m=1}^{12} EENS_m}{\sum_{m=1}^{12} L_m},$$

where $EENS_m$ and L_m denote respectively the Expected Energy not Supplied for the month m and the load for the month m . Using the values in Tables 4–5, the reliability indices for the two cases are found to be $EIR_y^1 = 0.8675$ and $EIR_y^2 = 0.8457$. Based on EIR_y values, the HSWPS that consists of $n = 1$ WT and the PVS with total area 163 m² is better. Clearly, the EENS and hence EIR_y values heavily depend on wind and solar regime of the location. Because the wind speed in the selected location is low and the solar radiation is relatively better, the HSWPS with single WT seems better in terms of reliability.

6. Summary and conclusions

In this paper, we have studied the performance of a hybrid system that consists of WTs and PVS in terms of reliability. In particular, we have analytically derived the distribution of the power output of the system by considering reliability values of WTs and the PVS. The theoretical distribution was then used to compute the EENS and EIR for the system under concern.

Since we have also derived the distribution of the power output of the HSWPS for more than one WT, our results generalize the results in Tina et al. [22]. Another novelty lies in the consideration of reliability values of WT and PVS in the performance assessment of the HSWPS.

As we have illustrated, the EENS and EIR values can be easily calculated after estimating the wind speed and solar irradiation distributions. Our results are general and can be used for any fitted wind speed and solar irradiation distributions.

The results of the paper can be effectively used for optimal design of the HSWPS before its construction. For example, we can determine the optimal number of WTs and the total area for the PVS based on the reliability index EIR and appropriately defined cost function. Manifestly, the costs of renewable energy components should also be considered in optimal decision making. This will be among our future research problems.

CRedit authorship contribution statement

Serkan Eryilmaz: Conceptualization, Methodology. **İrem Bulanık:** Computational details, Software. **Yilser Devrim:** Conceptualization, Methodology.

Declaration of competing interest

The authors declare that they have no known competing financial interests or personal relationships that could have appeared to influence the work reported in this paper.

Acknowledgments

This work was supported by The Scientific and Technological Research Council of Turkey (TUBITAK) under project TUBITAK 1001-119F182. The authors thank the anonymous referees for their helpful comments and suggestions, which were very useful in improving the paper.

Appendix

The proof of (11): Manifestly,

$$\begin{aligned}
 K(x) &= P \{ P_{WT} + P_{PV} \leq x \} \\
 &= \int_0^1 P \{ P_{WT} \leq x - s\eta_{PV} A_{PV} \} g(s) ds \\
 &= \int_0^1 Q(x - s\eta_{PV} A_{PV}) g(s) ds \\
 &= \int_{\max(0, \frac{x - P_r}{\eta_{PV} A_{PV}}}^{\min(\frac{x}{\eta_{PV} A_{PV}}, 1)} H(x - s\eta_{PV} A_{PV}) g(s) ds + \int_0^{\min(\frac{x - P_r}{\eta_{PV} A_{PV}}, 1)} g(s) ds. \quad (A.1)
 \end{aligned}$$

If $0 \leq x < P_r$, then from (A.1)

$$\begin{aligned}
 P \{ P_{WT} + P_{PV} \leq x \} &= \int_0^{\min(\frac{x}{\eta_{PV} A_{PV}}, 1)} H(x - s\eta_{PV} A_{PV}) g(s) ds \\
 &= \int_0^{\min(\frac{x}{\eta_{PV} A_{PV}}, 1)} \left[1 - F(v_{co}) + F \left(\left[\frac{x - s\eta_{PV} A_{PV}}{P_r} (v_r^3 - v_{ci}^3) + v_{ci}^3 \right]^{\frac{1}{3}} \right) \right] g(s) ds
 \end{aligned}$$

If $P_r \leq x < \eta_{PV} A_{PV} + P_r$, then from (A.1)

$$\begin{aligned}
 P \{ P_{WT} + P_{PV} \leq x \} &= \int_{\frac{x - P_r}{\eta_{PV} A_{PV}}}^{\min(\frac{x}{\eta_{PV} A_{PV}}, 1)} H(x - s\eta_{PV} A_{PV}) g(s) ds + \int_0^{\frac{x - P_r}{\eta_{PV} A_{PV}}} g(s) ds \\
 &= \int_{\frac{x - P_r}{\eta_{PV} A_{PV}}}^{\min(\frac{x}{\eta_{PV} A_{PV}}, 1)} \left[1 - F(v_{co}) + F \left(\left[\frac{x - s\eta_{PV} A_{PV}}{P_r} (v_r^3 - v_{ci}^3) + v_{ci}^3 \right]^{\frac{1}{3}} \right) \right] g(s) ds \\
 &\quad + G \left(\frac{x - P_r}{\eta_{PV} A_{PV}} \right).
 \end{aligned}$$

If $x < 0$ then $P \{ P_{WT} + P_{PV} \leq x \} = 0$, and if $x \geq \eta_{PV} A_{PV} + P_r$, then $P \{ P_{WT} + P_{PV} \leq x \} = 1$.

The proof of (23): For $x \geq 0$,

$$\begin{aligned}
 P \{ \max(L - P_h, 0) > x \} &= 1 - P \{ \max(L - P_h, 0) \leq x \} \\
 &= 1 - P \{ P_h \geq L - x \} \\
 &= \begin{cases} 0, & \text{if } L - x \leq 0 \\ 1 - P \{ P_h \geq L - x \}, & \text{if } 0 < L - x \leq P_{h \max} \\ 1, & \text{if } L - x > P_{h \max} \end{cases}
 \end{aligned}$$

Then,

$$\begin{aligned}
 EENS &= \int_{x \geq 0} P \{ \max(L - P_h, 0) > x \} dx \\
 &= \int_{\max(0, L - P_{h \max})}^L [1 - P \{ P_h \geq L - x \}] dx + \int_0^{L - P_{h \max}} 1 dx \\
 &= L - \int_0^{\min(L, P_{h \max})} P \{ P_h \geq u \} du.
 \end{aligned}$$

The proof of (24): Using (12) in (23), we have

$$\begin{aligned}
 EENS &= L - \int_0^{\min(L, P_{h \max})} [1 - p_1 p_2 K(u) - p_1(1 - p_2)Q(u) \\
 &\quad - (1 - p_1)p_2 R(u) - (1 - p_1)(1 - p_2)] du \\
 &= L - p_1 p_2 \int_0^{\min(L, P_{h \max})} (1 - K(u)) du + p_1 p_2 \min(L, P_{h \max}) \\
 &\quad - p_1(1 - p_2) \int_0^{\min(L, P_r)} (1 - Q(u)) du + p_1(1 - p_2) \min(L, P_{h \max}) \\
 &\quad - (1 - p_1)p_2 \int_0^{\min(L, \eta_{PV} A_{PV})} (1 - R(u)) du \\
 &\quad + (1 - p_1)p_2 \min(L, P_{h \max}) \\
 &\quad - (p_1 + p_2 - p_1 p_2) \min(L, P_{h \max}) \\
 &= L - p_1 p_2 \int_0^{\min(L, P_{h \max})} [1 - K(u)] du \\
 &\quad - p_1(1 - p_2) \int_0^{\min(L, P_r)} [1 - Q(u)] du \\
 &\quad - (1 - p_1)p_2 \int_0^{\min(L, \eta_{PV} A_{PV})} [1 - R(u)] du.
 \end{aligned}$$

References

- [1] Ceran B. The concept of use of PV/WT/FC hybrid power generation system for smoothing the energy profile of the consumer. Energy 2019;167:853–65.
- [2] Hamilton G, Smith DLJ, Bydder M, Nayak K, Hu H. Magnetic resonance properties of brown and white adipose tissues. J Magn Reson Imaging 2012;34(4):468–73.
- [3] Devrim Y, Bilir L. Performance investigation of a wind turbine–solar photovoltaic panels–fuel cell hybrid system installed at İncek region – Ankara, Turkey. Energy Convers Manage 2016;126:759–66.
- [4] Budak Y, Devrim Y. Comparative study of PV/PEM fuel cell hybrid energy system based on methanol and water electrolysis. Energy Convers Manage 2019;179:46–57.
- [5] Li YF, Zio E. A multi-state model for the reliability assessment of a distributed generation system via universal generating function. Reliab Eng Syst Saf 2012;106(2):28–36.
- [6] Spinato F, Tavner PJ, van Bussel GJW, Koutoulakos E. Reliability of wind turbine subassemblies. IET Renew Power Gener 2009;3:387–401.
- [7] Guo H, Watson S, Tavner P, Xiang J. Reliability analysis for wind turbines with incomplete failure data collected from after the date of initial installation. Reliab Eng Syst Saf 2009;94:1057–63.
- [8] Scheu MN, Kolios A, Fischer T, Brennan F. Influence of statistical uncertainty of component reliability estimations on offshore wind farm availability. Reliab Eng Syst Saf 2017;168:28–39.
- [9] Barros JJC, Coira ML, López, de la Cruz MP, del Caño Gochi A. Probabilistic life-cycle cost analysis for renewable and non-renewable power plants. Energy 2016;112(2):774–87.
- [10] Faza A. A probabilistic model for estimating the effects of photovoltaic sources on the power systems reliability. Reliab Eng Syst Saf 2018;171(1):67–77.

- [11] Hasan KN, Preece R, Milanović JV. Existing approaches and trends in uncertainty modelling and probabilistic stability analysis of power systems with renewable generation. *Renew Sustain Energy Rev* 2019;(101):168–80.
- [12] Kan C, Devrim Y, Eryilmaz S. On the theoretical distribution of the wind farm power when there is a correlation between wind speed and wind turbine availability. *Reliab Eng Syst Saf* 2020;(203):107115.
- [13] Adedipe T, Shafiee M, Zio E. Bayesian network modelling for the wind energy industry: An overview. *Reliab Eng Syst Saf* 2020;(202). Article 107053.
- [14] Acuña LG, Padilla RV, Mercado AS. Measuring reliability of hybrid photovoltaic-wind energy systems: A new indicator. *Renew Energy* 2017;(106):68–77.
- [15] Kamal Anoune K, Bouya M, Astito A, Abdellah AB. Sizing methods and optimization techniques for PV-wind based hybrid renewable energy system: A review. *Renew Sustain Energy Rev* 2018;93:652–73.
- [16] Moghaddam MJH, Kalam A, Nowdeh SA, Ahmadi A, Babanezdah M, Saha S. Optimal sizing and energy management of stand-alone hybrid photovoltaic/wind system based on hydrogen storage considering LOEE and LOLE reliability indices using flower pollination algorithm. *Renew Energy* 2019;(135):1412–34.
- [17] Devrim Y, Eryilmaz S. Reliability based evaluation of hybrid wind-solar energy system. *Proc Inst Mech Eng O* 2021;(235):136–43.
- [18] Louie H, Slougher JM. Probabilistic modeling and statistical characteristics of aggregate wind power. In: *Large scale renewable power generation, green energy and technology*. 2014, p. 19–51.
- [19] Villanueva D, Feijoo A. A review on wind turbine deterministic power curve models. *Appl Sci* 2020;(10):4186.
- [20] Pérez JMP, Márquez FPG, Tobias A, Papaelias M. Wind turbine reliability analysis. *Renew Sustain Energy Rev* 2013;23:463–72.
- [21] Raghuwanshi SS, Arya R. Reliability evaluation of stand-alone hybrid photovoltaic energy system for rural healthcare centre. *Sustain Energy Technol Assess*. 2020;(37):100624.
- [22] Tina G, Gagliano S, Rait S. Hybrid solar/wind power system probabilistic modelling for long-term performance assessment. *Sol Energy* 2006;(80):578–88.
- [23] Eryilmaz S, Devrim Y. Theoretical derivation of wind plant power distribution with the consideration of wind turbine reliability. *Reliab Eng Syst Saf* 2019;(185):192–7.